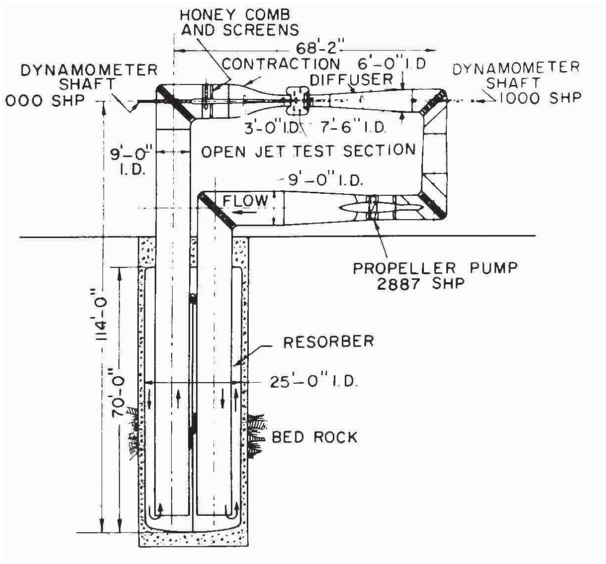

Figure 7b. DTMB 36-in. Water tunnel (1962)

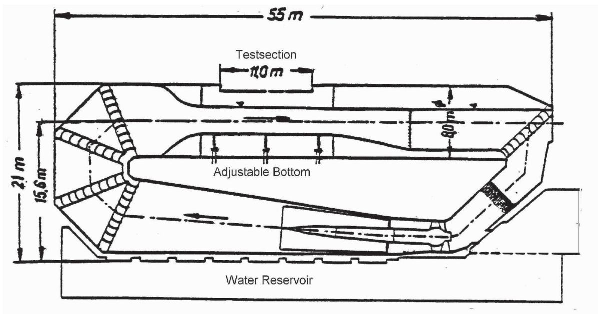

Figure 8. Circulating water tank UT2, VWS Berlin (1974)

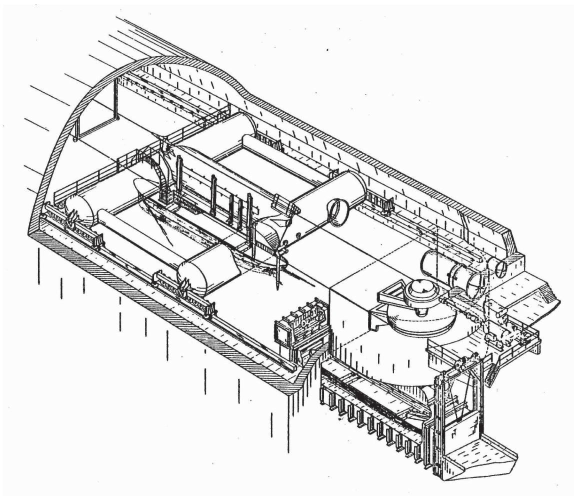

Figure 9. Depressurized towing tank of MARIN in Ede-Wageningen (1972)

the depressurized towing tank in Ede-Wageningen, Netherlands (Figure 9). The latter facility recently was modernized, e. g. the new carriage allows velocities up to 8 m/s instead earlier 4 m/s. Advantages of these facilities are the almost complete simulation of all components of the ship's wake and correct interaction between propeller and hull. Disadvantages are low propeller blade section Reynolds numbers and scale effects due to low nuclei and dissolved air content and also due to bubble dynamic scale effects with smaller dynamic pressures at Froude number of revolutions. Therefore, new developments try to unify the advantages of the free surface facilities , i. e. proper propeller inflow and interaction, with the advantages of conventional cavitation tunnels, i. e. high rate of propeller revolution, and additional treatment of the water for variable dissolved air and nuclei content. The new type of cavitation tunnels without free surface were erected in Sweden (1970), France (1988), Germany (1990), and USA (1991). Also in China and Korea recently two facilities of this type were built. Actually, the second HSVA tunnel from 1941 belonged already to this type of a cavitation tunnel, except for the gassing system. Since for navies noise problems at cavitating and cavitation-free conditions are important, the US Large Cavitation Channel LCC (Etter 2000) and the German Hydrodynamics and Cavitation Tunnel HYKAT got special hydroacoustic treatment (Pollmann/Lydorf 1991).

As exceptional hydroacoustic qualities of a cavitation facility require excellent flow behavior, respective hydrodynamic design considerations for the LCC and the HYKAT have been performed (Wetzel/Arndt 1994). In Figure 10a the velocity profiles of an air model for the HYKAT is shown (Arndt/Weitendorf 1990). It was found that the non-symmetry of the velocity profile was originated at the exit of the main diffuser and transmitted through the two following elbows without significant change. This original design resulted in a pump inflow condition that was unacceptable (Figure 10b). Considerable improvement of the inflow to the pump was achieved with design angle for the turning vanes in the first and 1.5° less for the vanes in the second elbow. A mathematical model supported endeavors for improvement so that finally a fully acceptable inflow was reached (Figure 10b). The first trial runs of the HYKAT showed a better cavitation behavior of the impeller than specified. - Figure 11 shows the elevation of the HYKAT having a test section of 2.8 m by 1.6 m and maximum speed of 12 m/s. The pressure in the test section can be varied between 0.25 and 2.5 bar. During the design of the HYKAT an evaluation of existing and planned cavitation facilities was undertaken that included flow quality, correlation of model cavitation to full scale, flow rate ($Q \geq 20\ m^3/s$ for $V \geq 5 m/s$), measurement features and hydroacoustic qualities (Weitendorf, Friesch, Song 1987).

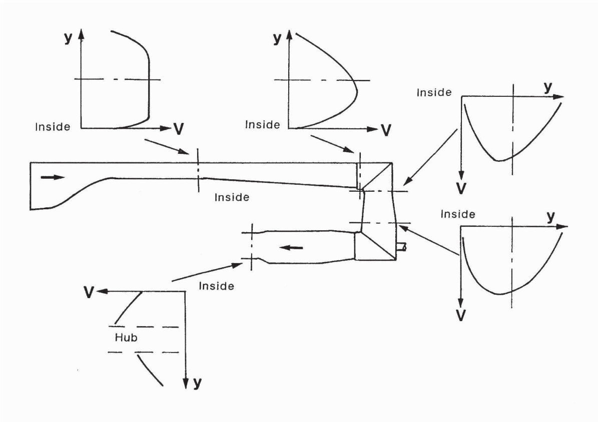

Figure 10a. Vertical plane velocity profiles in air HYKAT model according to Arndt et al. (1990)

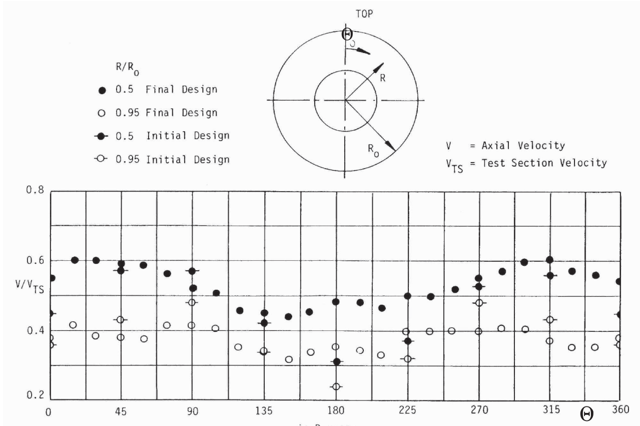

Figure 10b. Measured axial pump intake velocities for initial and final HYKAT design; Wetzel/Arndt (1994)

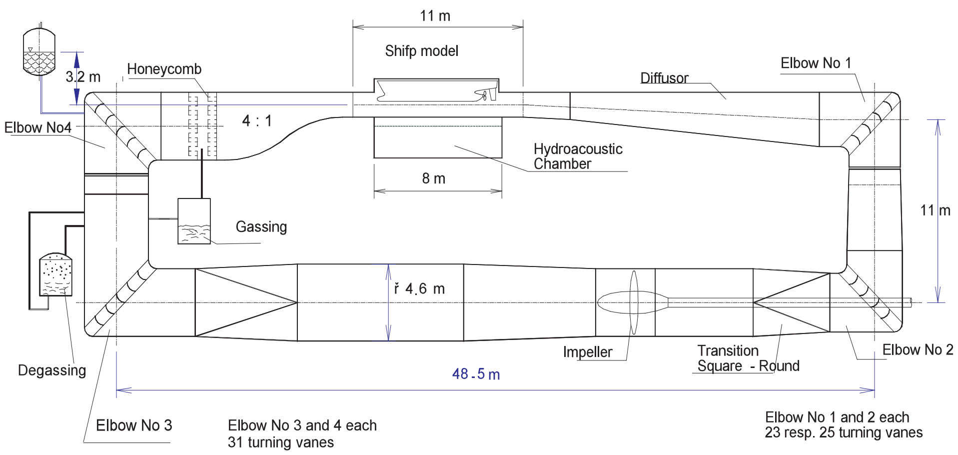

Figure 11. Hydrodynamics and Cavitation Tunnel HYKAT of HSVA (1990)

Further, there are cavitation test facilities with free surfaces for propeller tests, e. g. at KAMEW A in Kristinehamn, Sweden, and at the Technical University Berlin, Germany, and several others (Etter 2000).

4. On Similarity Laws and Test Rules

Besides geometrical similarity, the velocity prediction from model M to full scale FS requires either equal Froude numbers Fr for both , i. e. equal relation between inertia and gravity for M and FS (Froude 1855, republished 1955), or equal Reynolds numbers Re (Reynolds 1883), i. e. the relation between inertia and friction; these numbers are:

$$Fr = \frac{V}{\sqrt{g \cdot L}} \quad \text{as well} \quad Re = \frac{V \cdot L}{\nu}$$

with V = velocity, L = ship length (or propeller-diameter), g = gravity and ν = kinematic viscosity. Since the length L in the numbers stands either in denominator of the Fr- or the numerator of the Re-number; therefore, the Froude law is preferred when gravity is predominant.

At the early 20th century D.W. Taylor (1906) stated that the general law of similarity according to Newton's law is also valid for propellers. This allows the definition of coefficients, e. g. equal thrust coefficients for M and FS:

$$K_T = \frac{T}{\rho n^2 D^4}$$

with n the rate of revolution, D the diameter, and the equal advance coefficient

$$J = \frac{V}{n \cdot D}$$

guaranties the similarity of the velocity triangles for M and FS.

In his second tunnel Parsons simulated the velocities according to Froude's Law (Burril 1951). At that time the propeller loading was set by the apparent slip

$$s_s = \frac{n \cdot H - V_s}{n \cdot H}$$

with n = the rate of revolution, H = the pitch and V_S = the ship speed. Successful propellers showed a slip s_S = 0.10 to 0.12.

In both tunnels Parsons did not yet use an independent pressure setting. In the first tunnel the atmospheric pressure above the heated water was removed by an air pump and in the second the maximum attainable vacuum of 0,45 lbs/inch² (30 mbar absolute pressure) for the static head above the propeller was always applied in the vacuum chamber above the test section (Burrill 1951). Remarkable results have been achieved by this method, however by wide variation from s_S = 0.08 to 0.28 (see Cook's discussion to Kempf/Lerbs 1932 with face side cavitation in model corresponding to the erosion pitting of the "Bremen" propeller in Figure 13).

After Weber (1930) had shown the General Similarity Principle of Physics that includes Newton's similarity for constant J- and K_T-values and more over Ackeret (1930) proved the constancy of the cavitation numbers σ for M and FS the model tests in the first HSVA cavitation tunnel were based on these rules . This new procedure compared to the one based on Froude's law resulted in vivid discussions and concern to the Kempf/Lerbs paper (1932) at the Institution of Naval Architects (INA). But finally it found general acceptance lasting til today.

Later Lerbs (1944)showed by further similarity tests that the air content (nowadays recognized as total air content of water) had no influence on the steady values of thrust and torque. Also, he verified that these steady values at propeller cavitation tests above the critical Reynolds number of $Re_{crit} \approx 0{,}8 \bullet 10^5$ as well with 8 to 9 % different local cavitation numbers are neglectably influenced through scale effects. This almost classical procedure by Lerbs for steady values should also deserve application for unsteady values, as e.g. cavitation noise and vibration exciting pressure fluctuations above the propeller. In this connection micro bubbles as cavitation nuclei for equal model and full scale cavity are relevant. Several authors have suggested a rule for nuclei seeding following the third power of the model scale $\lambda = A_{orig}/A_{mod}$ (see ITTC Cavitation Committee Rep. 1987, p.169). A rule derived from the Rayleigh-Plesset-equation by Isay (1981) reads: $(\varsigma_{0j}A^3)_{Mod} = (\varsigma_{0j}A^3)_{Orig}$, where A is half the profile length and ς_{0j} the nuclei concentration for the individual bubble radii class j. Looking at this rule that requires a considerably higher nuclei concentration in model than in full scale the inclusion of resorbers into the flow circuit of cavitation tunnels does not seem to be reasonable.

Recently the noise level excited by unsteady cavitation received some significance not only for navy vessels but also for cruise liners and ferries. A summary of the rules for respective noise measurements and predictions of the prototype at cavitating conditions that account for the nowadays knowledge has been given by Baiter and Blake (1991).

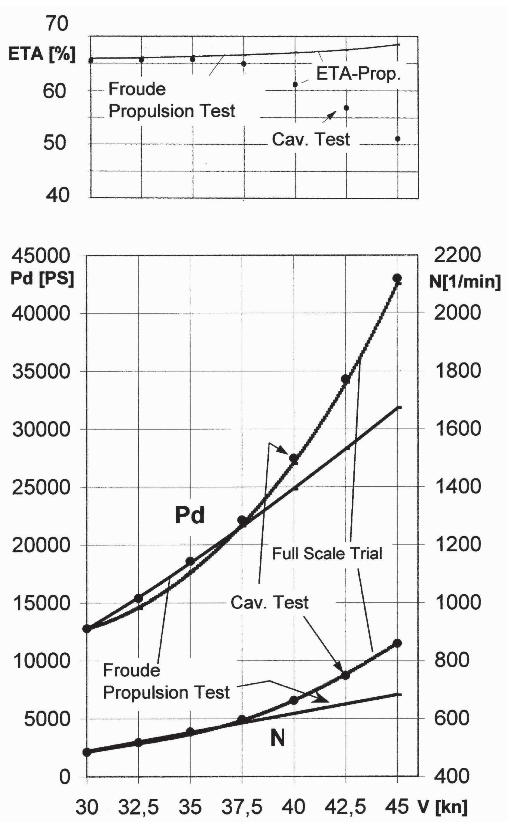

Figure 12. Results from cavitation test, Froude propulsion test, and full scale trial test according to Lerbs (1944)

5. On the Cavitation Effects Thrust Breakdown, Erosion, Vibration, and Noise

When covering at least 70% of the total blade area of the propeller with cavitation, thrust breakdown occurs. This is due to constant vapor pressure at the blades instead of the quadratic thrust dependance on the velocity at cavitation-free condition. Lerbs' similarity investigations (1944) led also to test and prediction rules for heavily cavitating conditions. Such a result for a navy vessel is shown in Figure 12. The values power Pd, rate of revolution N, and propeller efficiency ETA from the towing tank at Froude condition have been corrected by cavitation tunnel results The excellent agreement in Figure 12 proved the above described procedure for tests also with fully cavitating propellers.

A resolute pursue of the thrust breakdown problem at heavily cavitating conditions led to the development of a theory for fully or super cavitating profiles (Wu 1955; Tulin 1955) and propellers whose efficiencies approached those of non-cavitating screws (Newton/Rader 1960). In the former Soviet-Union Pozdjunin proposed a special "supercavitating" propeller with wedge profiles already in 1938. Tulin

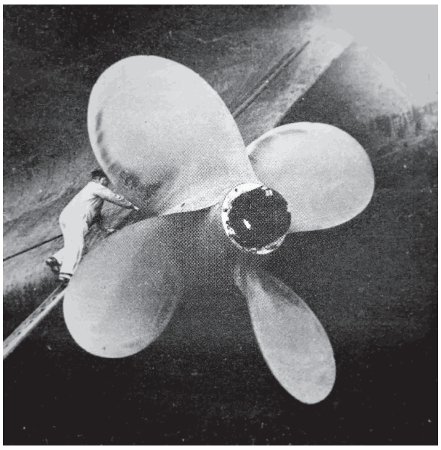

Figure 13. Erosion pitting on face of the “Bremen” propeller (1928)

(1964, 2001) gave recently a summary on this subject.

The cavitation erosion problem on propellers was first tackled by Parsons/Cook (1919) and Raleigh (1917) almost simultaneously developed the theory on the behavior of a cavitating bubble in ideal fluid. Parsons and Cook found that the “erosive action ... of shock pressures as high as 180 tons per sq. in. ... was in main not chemical but mechanical in action”; Parsons said 1919: “The erosion was due to the intense blows struck upon the blades by the nuclei of the vacuous cavities closing up against them...” (Burrill 1951). The research by Lerbs on cavitation eliminated the erosion problem at the face side of the propellers of Atlantic liner “Bremen” (Figure 13). This was achieved by “cutting back the leading edge, and increasing the turn-up on the driving face ...” (Burrill 1951, p. 165).- Regarding the erosion problem extremely important for the practical shipbuilding the 13th Cavitation Committee of the ITTC (Emerson 1972) stated that two types of cavitation are mainly responsible for the pitting on the blades: Bubble and cloud cavitation. Recently obviously fluctuating sheet cavitation and unstable tip vortex cavitation seem to contribute to the erosion damages on the propellers of container ships whose speeds steadily increase.

Before, during, and immediately after World War II cavitation research was mainly focused on steady aspects of the problem, yet later on, investigations disclosed the influence of unsteady cavitation on vibration and noise excitations of ships. Whereas vibration research was originally merely concentrated on the propeller bearing forces, the propeller surface forces were touched by a report from Denny (1967) containing the influence of cavitation on pressure fluctuations above the propeller. The significance of this influence was neither recognized by Denny’s experiments nor the first theory on the hydroacoustics of cavitating screw propellers (Isay 1967). The importance of cavitation on pressure fluctuations became clear when the experiments by Van Oossanen/Van der Kooij (1972) and the work by Huse (1972) were published. In Figure 14 three different cavitation patterns according to Huse’s calculations are plotted. The upper pattern shows a cavity thickness τ = 10 % of the chord length being constant for one revolution and leading to the pressure amplitude K_{P1}. The pattern in the middle with unstationary cavitation called cavity volume variation corresponds to an amplitude $K_{P2} = 4K_{P1}$. The lower pattern with shortest cavitation duration results in $K_{P3} = 10K_{P1}$. The reason for the strongly increasing amplitude K_P is the displacement effect of the unstationary cavity volume that follows the second derivative of the time respective blade position α:

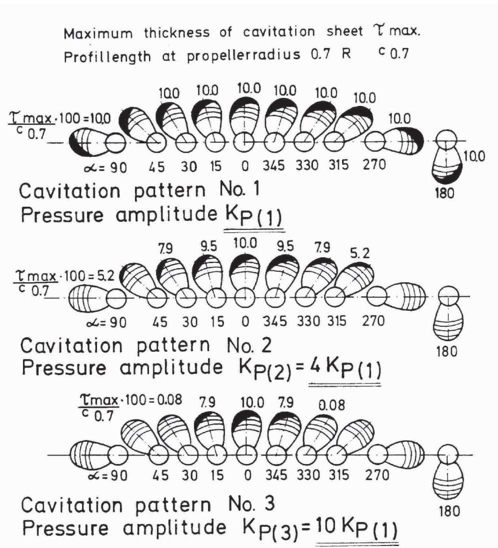

Figure 14. Effect of cavity volume variation - Calculated pressure amplitudes for three cavitation patterns according to Huse (1972)

$$K_p \propto \frac{\partial^2 V_{Kav}}{\partial\, \alpha^2} \;;$$

Moreover, evenly distributed phases at different positions on the ship’s surface and the increase of pressure amplitudes in case of cavitation create an enhancement of the resulting force compared to the cavitation-free condition. In case of a six bladed propeller the resulting force for the lower row in Figure 14 is 135 times larger than fo the upper one with no cavity volume variation. This shows why the surface forces contribute much more to propeller-generated vibrations than the bearing forces.

Concerning acceptable propeller-excited pressures (abt. 4 to 8 kPa for the blade frequency, recently for cruise liners much smaller) and vibrations there are full scale measurements (e. g. Holden 1979; ITTC 1987; Weitendorf 1989; Friesch 1998). When pressure fluctuations have been predicted from model tests scale effects may occur (Weitendorf 1989). Figure 15a shows that the pressure amplitudes $K_P = \Delta p/(\rho n^2 D^4)$ of the “Sydney Express”-model from the medium HSVA tunnel depend on the oxygen content O_2 of water (in % saturation at atmospheric pressure) and on the rate of revolution. Further, the oxygen content O_2 is related to the spectrum of nucle air bubbles (Weitendorf/Tanger, 1999). For rates of revolution $n \geq 20$ Hz (in Figures15a: n = 22,5 u. 32 Hz) and an O_2-saturation > 50 - 60% the amplitudes ($K_P \approx 0{,}03$) agree satisfactorily with full scale. Already earlier investigations

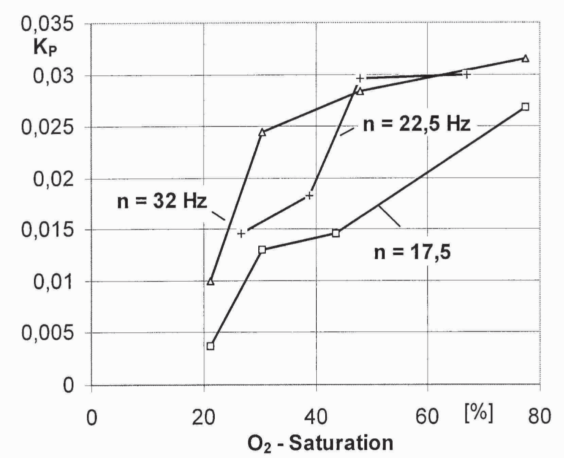

Pressure pick-up P7; $K_T = 0.175$; $\sigma_n = 0.185$

Figure 15a. Pressure fluctuations of "Sydney Express" propeller in medium HSVA tunnel depending on oxygen saturation of the water

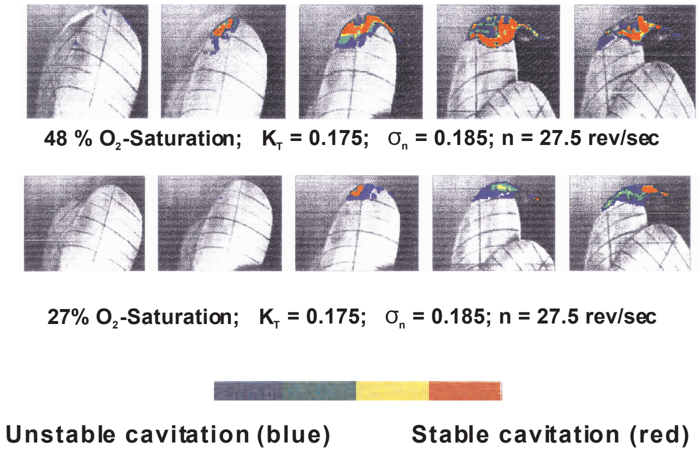

Figure 15b. Cavitation extent for "Sydney Express" propeller in medium HSVA tunnel at different oxygen content

(Keller/Weitendorf 1975) showed the dependance of pressure amplitudes K_P on rate of revolutions and small nuclei bubble content. The reason for this fact is mainly the weak absolute minimum pressure at the profile for the creation of cavitation at small rates of revolution, i.e. bubble dynamic scale effects. Respective numbers will be shown later. The extent of cavitation at different air content exciting small or higher amplitudes as in Figure 15a is given in Figure 15b. Detailed explanations on the occurrence and intermittence as well on repeatability of the cavity extent in model tests by video camera and computer analysis and its documentation by colors (red corresponds to so-called stable and blue to unstable cavitation) are presented in a paper by Weitendorf/Tanger (1992). Figure 15b shows that the low O_2-content of 27% (lower row) leads to smaller cavity extent and stronger intermittent (or unstable) cavitation than the higher one (upper row). - Further scale effects at model tests, e. g. those by Reynolds effects or by the ship's wake are discussed by Isay (1984) and Blake et al. (1990).

Besides the prediction of blade frequency pressure amplitudes recently also the higher blade frequencies became important as well broad band noise (Raestadt 1996; Friesch 1998). In this connection the pronounced tip vortex break down in front of the rudder (Figure 2d and e) gets more attention (English 1979). In cases without rudder thick tip vortices with nodes (Figure 2c) have excited higher blade frequency amplitudes (Weitendorf 1973, 1977). Recently carried out tests in full scale and model for passenger ships showed that tests with whole ship models in large tunnels resulted in good correlations (Friesch 1998, ITTC-Reprts 1996, 1999), even for higher blade frequencies, as Figure 16 displays. -

Latest results to this field are high speed videos that allow correlations between cavitation phenomena and propeller-generated pressure amplitudes (Johannsen 1998).

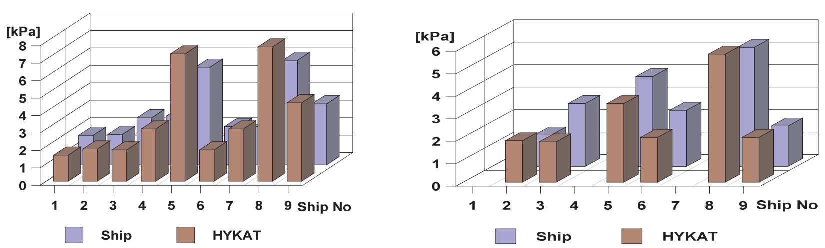

Blade Frequency **Second Blade Frequency**

Figure 16. Model - Full scale correlation of pressure fluctuations above propeller as effect of cavitation